We are IntechOpen, the world's leading publisher of Open Access books Built by scientists, for scientists

Modelling of HDD head positioning systems regarded as robot manipulators using block matrices

Tomasz Trawiński and Roman Wituła
Silesian University of Technology
Poland

1. Introduction

The modern hard disk drive (HDD) head positioning systems may be regarded as excellent example of mechatronics systems consisting of different components – subsystems: electrical (driving motors – actuators, flexible printed circuits, writing and reading heads etc.), mechanical (bearings, air bearings, swing arm, suspensions etc.) and electronics (power amplifiers, control system etc.). In this chapter we will focus only on the mechanical system of head positioning system, which usually consist of following components: main swing arm (so-called E-block) fixed with moving coil of the VCM (voice coil motor) motor, suspensions of the sliders, sliders with writing and reading heads. All of these elementary components (assumed to be stiff and rigid enough) are connected to each other and these connections may be treated as rotary or prismatic joints. Modern head positioning systems, beside fundamental VCM motor (which plays the role of fundamental source of driving torque), are equipped with additional micro-actuators for better track tracing or rejection of the internal and external disturbances. Usually the head positioning systems equipped with auxiliary micro-actuators are called as dual-stage (DS) positioning system. The dual-stage positioning systems may be classified according to kinds of auxiliary micro-actuators and place where the macro-actuators are attached to kinematic chain of head positioning system. For auxiliary micro-actuators very often the PZT (piezoelectric) micro-actuators or electrostatic MEMS (micro-electro-mechanical systems) micro-actuators are used. PZT micro-actuators are often placed between and tip of E-block and the beginning of slider and head suspension (Rotunno et al., 2006) and actuate the suspension or play the role of the sensor for vibration sensing (Huang et al., 2005), or they are placed between suspension and slider and drive slider directly (Hong et al., 2006). The MEMS micro-actuator in HDD head positioning systems, for the sake of relatively small dimensions and small generated forces (torque), are put between suspension and slider (drive slider directly) or they are placed between slider and heads (drive the heads directly). Some different and very interesting ideas for direct drives of HDD heads is presented in (Schultz, 2007), where thermal expansion of head pole tip is used for approaching the head to disk surface during write process. All presented mathematical models of head positioning systems are prepared for analysis of its cooperation only with one side of data disk. Some of proposed mathematical models take into account mutual interactions between auxiliary micro-actuator and main VCM motor, but they do not take into account this mutual interactions when positioning system is equipped with more then one micro-actuator. In this chapter mathematical model of head positioning system cooperating with more then one side of data disk will be derived. Firstly the real kinematic structure of HDD positioning system will be decomposed into elementary joints and links, that allows writing them in terms of open kinematics chain of small robot manipulators. Next the kinematic chains will be extended to multilayer kinematics chains. Secondly for multilayer kinematic chains of positioning system (using commonly known mathematical methods used in robot dynamics) mathematical model will be formulated and written in terms of Lagrange equations. During the mathematical model formulation the block matrix will be used for inverting the dynamics matrix of head positioning system. Finally the general method for dynamic matrix inversion for more complicated kinematic chains of positioning system will be given and carefully discussed.

2. Kinematic structure of HDD positioning system

2.1 Exemplary modern head positioning systems

The mechanical construction of head positioning system is strongly related with data areal density. Data areal density denotes the amounts of data which may be stored on unit area of data disk, and it is expressed in gigabits per square inch (Gb/in^2). Nowadays the data areal density in HDD reaches values up to several hundreds of Gb/in^2 (Trawiński & Kluszczyński 2008). For small areal densities (less then few tens of Gb/in^2) and resulting relatively width data track, the commonly used structures of HDD positioning systems were equipped with only one driving motor – VCM motor. Such a system forms one degree of freedom (1 DoF) mechanical system, usually equipped with massive E-block. Basic structure of positioning head system is presented in Fig.1; this positioning system operates with data areal densities reaching 15 Gb/in^2.

Fig. 1. Head positioning system for low data areal densities

In the Fig. 1 the numbers in the circles denote: (1) – E-block, (2) – sliders and heads suspensions, (3) – flexible printed circuit, (4) – VCM motor armature coil, (5) – pivot. This positioning system cooperated with spindle system consisting of set of three data discs. Another example of head positioning system which cooperates with data areal densities reaching 50 Gb/in^2 is presented in Fig. 2. Number in circles denotes this same part of positioning system like this presented in Fig. 1.

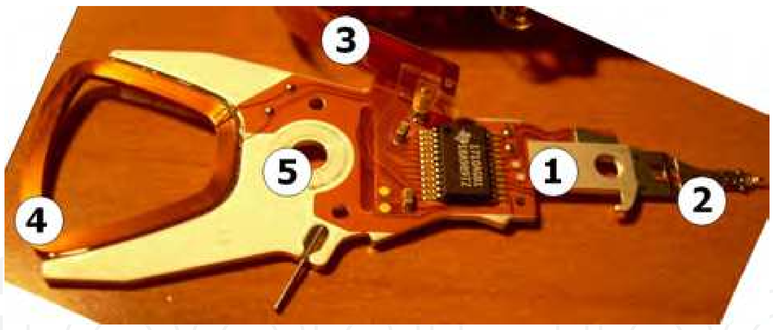

Fig. 2. Head positioning system for medium data areal densities

It is easy to spot that system presented in Fig. 2 is ready to cooperate only with one side of data disc. Basing on this two discussed positioning system it is very difficult to eliminate or suppress all internal disturbances such like: suspension air induced vibration, pivot nonlinearities, structural resonances of E-block, repeatable run-out (RRO) and non-repeatable run-out (NRRO) of data track due to rotation of spindle system (Wang & Krishnamurthy, 2006). This problem may be solved for example by utilising auxiliary macro-actuators or improvements in control system. (Chen & Horowitz, 2001) for this reason were proposed the silicon actuated suspension over PZT and achieved range of head motion (generated by PZT micro-actuator) about ±1.3 μm at ±30 V supply. In Fig. 3 exemplary and simplified view of PZT micro-actuator for suspension actuation (which is placed between end tip of E-block and beginning of suspension) is presented (Jiang et al., 2007), (Rotunno et al., 2006).

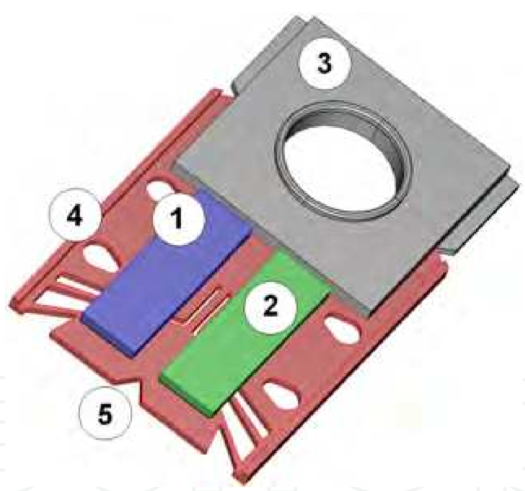

Fig. 3. Exemplary PZT micro-actuator for suspension actuation

In Fig. 3 the numbers in the circles denote: (1) and (2) – PZT stripes acting (extends) in opposite directions under voltage supply, (3) – end tip of E-block, (4) – flexible part - gimbals, (5) – place for suspension attaching.
Another example of PZT actuated suspension is presented in (Koganezawa & Hara, 2001) but this time the sheer-mode PZT where used to generate head motion. They achieved the motion of head in range of ± 0.5 μm at ± 30 V supply.
Placing the PZT micro-actuator between suspension and end tip of E-block may result (during PZT operation) in structural resonance excitation in suspension, thus certain

proposition in (Hong et al. 2006) was given for direct drive of the slider. Exemplary view of PZT actuated slider is presented in Fig. 4.

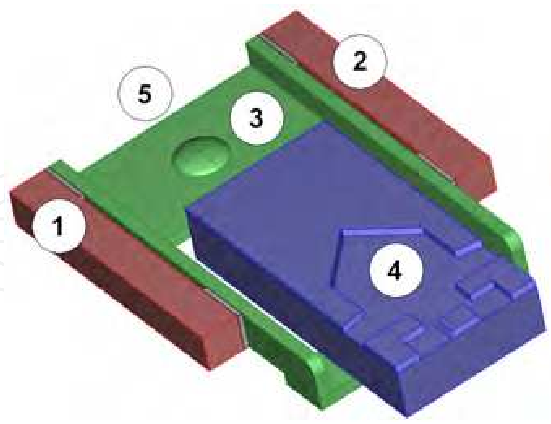

Fig. 4. Exemplary PZT actuated slider

In Fig. 4 the numbers in the circles denote: (1) and (2) – PZT stripes which are bending under voltage supply, (3) – flexible part – gimbals, (4) – slider, (5) – place for suspension attaching.
Using higher rate of sampling frequencies in servo system, reducing NRRO and RRO, reducing air induced vibration due to spoiler (attached over spinning disk) is possible to push the border of areal density when the auxiliary actuation will be inevitable (Sugaya, 2006).

2.2 Decomposition of head positioning system into joints and links

The mechanical subsystem of head positioning system, as it was mentioned before, may be represented as a set of stiff links connected by rotary or prismatic joints with one degrees of freedom. In chosen joint may act torque (or forces) generated by main motor and auxiliary micro-actuators. Such a set of links and joints is very similar to kinematic chain of small robot manipulators. But the fundamental difference is in range of motions arising in every joints. In the robot manipulators joints the ranges of motion are usually high and almost equal to each other. In case of head positioning systems the angular rages of joint motions differ very much. Motion of the main joint usually covers the angle between 30 to 40 degrees for 3.5 inch disk drives, for smaller drives equipped with 2 inch disk (or smaller in diameter) the range of angular motion may by smaller then 30 degrees. For another joints the values for angular motion are small (usually few degrees or fraction of degree or micro-degree, except (Sarajlic et al., 2009)) and depending on kind of auxiliary micro-actuator and its place in kinematic chain (Sarajlic et al., 2009). For these reasons we may assume forgoing correlation between real parts of head positioning system and hypothetical robot manipulator kinematic chain:

- the fundamental kinematic pairs consist of HDD frame and housing, E-block and VCM armature coil which are connected by rotating joint (pivot). On this joint act torque generated by VCM motor and torque (force) generated by flexible printed circuit (this effects will be further omitted for simplicity). The first rotary joint will be treated as perfect rotary joint (with one degrees of freedom) without any nonlinearities (this is very serious simplify assumptions). Problem of pivot nonlinearities is discussed in

(Ohno & Horowitz, 2005). The fundamental link (HDD frame and housing) will be called as “base” and second link (E-block, VCM coil) will be called as “bough”.

- The second kinematic pair consists of E-block and suspension connected with rotary joint. On this joint may acts torque (force) generated by PZT micro-actuator or alternatively spring torque (force), because connection between E-block and suspension is flexible in predominant cases.
- The third kinematic pair consists of suspension and slider which are connected by gimbals, but this kind of connections may be alternatively regarded as rotary or prismatic. Slider forms the fourth link.
- The fourth kinematic pair consists of slider and heads (reading head – magneto-resistive and writing heads – electromagnetic) connected to each other by means of prismatic joint. The set of heads forms the fifth link.

All links from third to fifth constitute the “branch” links. Number of links belonging to branch may vary and it depends on simplification made on kinematic chain of head positioning system. In illustrative way, the correlations between parts of real head positioning system and its robot manipulator kinematic chain equivalent representation is shown in Fig. 5.

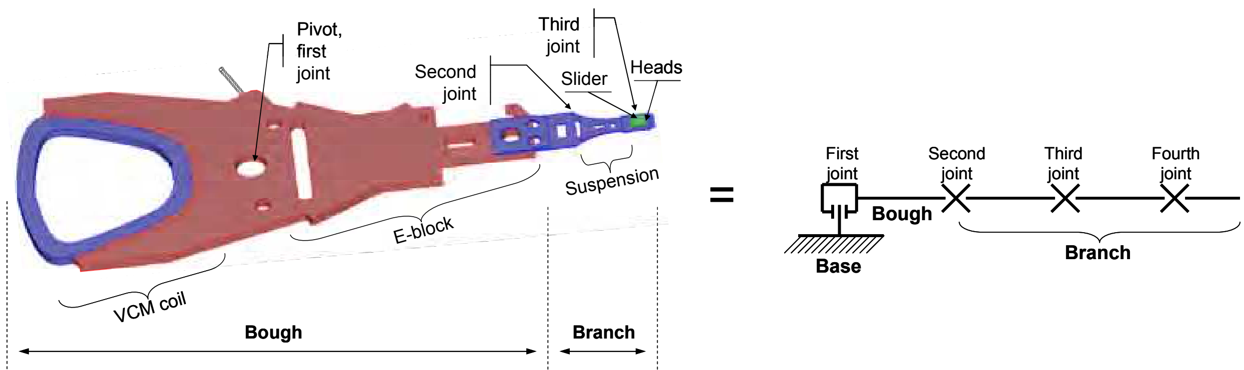

Fig. 5. Positioning system represented as manipulator

On the right side in Fig. 5 the simplified kinematic chain diagram is presented. The signs “x” denote joints which may be either rotating or prismatic. The first joint (in Fig.5) is rotating with rotating axis lie in the plain of drawings (and it is perpendicular to the bough). Basing on this schematic representation same kinematic chains of head positioning system presented in (Huang & Horowitz, 2005) may be represented in forthcoming figures. The head positioning system presented in (Huang & Horowitz, 2005) uses two sources of torque (force), one generated by VCM motor and the second (force) is generated by MEMS micro-generator (which drives directly the slider), so the simplified schematic representation of this manipulator is presented in Fig.6 and consists of two rotary joints (with rotating axis perpendicular to each other) and one prismatic joint (represented MEMS actuated slider). The second joint with rotating axis perpendicular to the plain of page is, in Fig.6, denoted by circle. The square with cross inside denotes, in Fig. 6, the prismatic joint.

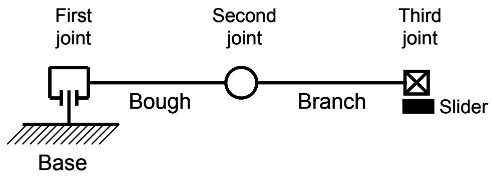

Fig. 6. Manipulator with 3 degrees of freedom

In Fig.6 in first joint acts VCM motor but second joint is not actuated – this is passive joint (Trawiński, 2007). The schematic representation of manipulator of positioning system which may be constructed basing on (Sarajlic et al., 2009) is presented in Fig. 7.

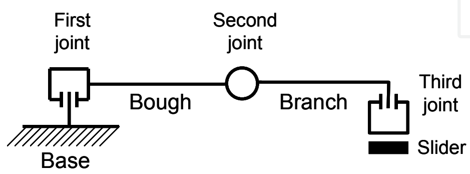

Fig. 7. Manipulator with 3 degrees of freedom

Kinematic chain of above mentioned manipulator consists of three rotating joints. The last rotating joint is driven by electrostatic MEMS 3-phase stepper motor (Sarajlic et al., 2009). This solution allows to compensate skew of reading and writing heads (Sarajlic et al., 2009). The second joint, as it was in previous case, is not actuated.

2.3 Multilayer head positioning system

Most of presented and known mathematical models of head positioning system assume its cooperation only with one side of data disk. It allows for analysis of internal dynamic interaction between parts of positioning systems, but does not take into consideration mutual interactions between multiple sets of suspensions and heads which cooperate with other sides of data disk. These mutual interactions may be shown only when the kinematics chain will be extended by another suspensions, sliders and heads which cooperate with the other sides of data disk. In our simplified schematic representation, presented in Figs. 6 & 7, for preparing them to cooperate with two sides of data disk, we have to add another branch. If it is done the schematic representation of kinematic chains look like these presented in Fig.8.

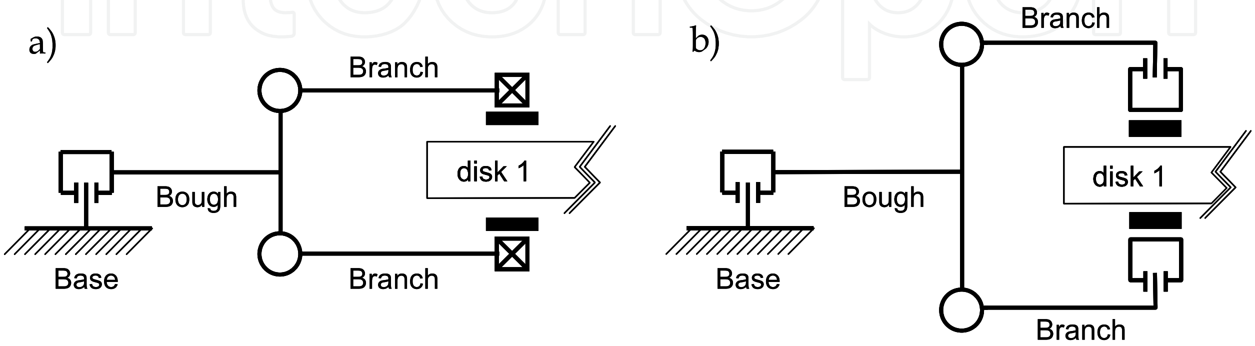

Fig. 8. Schematic view of positioning system manipulators capable of cooperation with two sides of data disk

When the head positioning system cooperates with set of two disk, and each side of disks is in use for data storing, then simplified kinematics chain will consist of four branches. Similarly for more additional disk the number of branches increases gradually for two branches for each disk. The positioning system now consists of multiple layer, one layer include single branch and one disk side. Such positioning system with multiple number of layers included branches, disk sides and bough will be further called as multilayer head positioning system. The individual branches, which belong to different layers, will be denoted by small letters starting from "a", every link of chosen branch will be assigned by number (starting form "2" upwards) and letter coincide with branch sign. The joints belonging to chosen branch will be denoted by letter coincide with the sign of branch and number (starting from "2" upwards). Bough link will be denoted by "1" and first joint by "(1)". The simplified schema of exemplary multilayer head positioning system, with symbols of branches etc., is presented in Fig. 9.

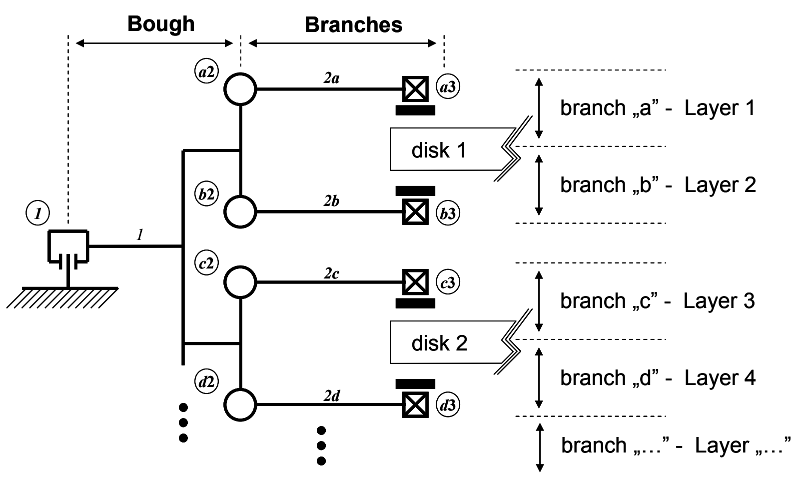

Fig. 9. Simplified schema of multilayer manipulator

For further consideration the multilayer kinematics chain presented in Figs. 8a) & 9 will be chosen, on its background the mathematical model will be formulated. The analysis of kinematics chains presented in Figs. 7 & 8.b) is discussed in (Trawiński & Kluszczyński, 2008).

3. Mathematical model of multilayer head positioning system

3.1 Dynamics matrix formulation

In matrix notation the Lagrange equations are given by:

$$\mathbf{D}\ddot{\mathbf{q}} + \mathbf{C}\dot{\mathbf{q}} + \mathbf{G} = \boldsymbol{\tau} \tag{1}$$

here and subsequently $\mathbf{D}$ – denotes dynamic matrix, $\mathbf{C}$ – centrifugal and Coriolis force matrix, $\mathbf{G}$ – gravitational forces and torque, $\boldsymbol{\tau}$ – driving torque vector, $\mathbf{q}$ – vector of generalized displacements.

The Lagrange equation is a set of second order differential equation, and for convenient calculation should be rewritten into normal form:

$$\dot{\boldsymbol{\omega}} = \mathbf{D}^{-1}(\boldsymbol{\tau} - \mathbf{C}\boldsymbol{\omega} - \mathbf{G})$$
$$\dot{\mathbf{q}} = \boldsymbol{\omega} \tag{2}$$

which consist of the set of two first order differential equations (second set is related with generalized speeds). In equations (1) and (2) is present the dynamic matrix, which can be derived from kinetic energy of whole multilayer head positioning system. The kinetic energy of this system may be expressed in quadratic form which include the dynamic matrix, as follows:

$$T = \frac{1}{2}\dot{\mathbf{q}}^T \mathbf{D}\dot{\mathbf{q}} \tag{3}$$

When motion analysis of "j" – link will be carried out according to its centre of masses, then kinetic energy may be expressed in sun of two terms – translational and rotational terms of kinetic energy, therefore whole kinetic energy is equal to:

$$T = T_L + T_R = \frac{1}{2}\sum_j m_{cj}\mathbf{v}_{cj}^T\mathbf{v}_{cj} + \frac{1}{2}\sum_j \boldsymbol{\omega}_{cj}^T\mathbf{I}_{cj}\boldsymbol{\omega}_{cj} \tag{4}$$

where T_L, T_R – denote translational and rotational terms of kinetic energy respectively; m_{cj} – mass of the link concentrated in his mass centre; $\mathbf{v}_{cj}$ – vector of linear speed; ω_{cj} – vector of angular speed of mass centre; $\mathbf{I}_{cj}$ – mass moment of inertia of link at mass centre.
The vector of linear speed occurring in equation (3) may be expressed in terms of the jacobian matrices, which describes the relation between joint generalised velocities and velocities of centre of masses expressed in coordinate system fixed with the base, thus:

$$\mathbf{v}_{cj} = \mathbf{J}_{vcj}\dot{\mathbf{q}} \tag{5}$$

where $\mathbf{J}_{vcj}$ – jacobian matrix of linear speed,
and for angular rotating speed, we have:

$$\boldsymbol{\omega}_{cj} = \mathbf{R}_{cj}^T\mathbf{J}_{\omega cj}\dot{\mathbf{q}} \tag{6}$$

where $\mathbf{J}_{wcj}$ – jacobian matrix of angular speed; $\mathbf{R}_{cj}$ – matrix of rotation (part of homogenous transformation matrices) of chosen link mass centre.
For jacobian matrices calculation and homogenous transformation matrices related with head positioning system refer to (Trawiński, 2007). Substituting (5) and (6) into equation (4), for "j" links of total "m" number of links (their centre of masses) of multilayer head positioning system, one may write:

$$T = \frac{1}{2}\dot{\mathbf{q}}^T\sum_{j=1}^{m}(m_{cj}\mathbf{J}_{vcj}^T\mathbf{J}_{vcj} + \mathbf{J}_{\omega cj}^T\mathbf{R}_{cj}\mathbf{I}_{cj}\mathbf{R}_{cj}^T\mathbf{J}_{\omega cj})\dot{\mathbf{q}} \tag{7}$$

The above derived equation may be expressed in terms of bough kinetic energy component and branches kinetic energy components:

$$T = \frac{1}{2}\dot{\mathbf{q}}_0^T\{m_{c1}\mathbf{J}_{vc1}^T\mathbf{J}_{vc1} + \mathbf{J}_{\omega c1}^T\mathbf{R}_{c1}\mathbf{I}_{c1}\mathbf{R}_{c1}^T\mathbf{J}_{\omega c1}\}\dot{\mathbf{q}}_0 + \frac{1}{2}\sum_g \dot{\mathbf{q}}_g^T\{\sum_{j=2}^{n}(m_{cj}\mathbf{J}_{vcgs}^T\mathbf{J}_{vcgs} + \mathbf{J}_{\omega cgs}^T\mathbf{R}_{cgs}\mathbf{I}_{cgs}\mathbf{R}_{cgs}^T\mathbf{J}_{\omega cgs})\}\dot{\mathbf{q}}_g \tag{8}$$

where m_{c1}, m_{cj} – masses of bough and "j" links of branches; $\mathbf{J}_{vc1}$, $\mathbf{J}_{vcj}$ – (3×n) dimensional jacobian matrices of linear speed; $\mathbf{J}_{wc1}$, $\mathbf{J}_{wcj}$ – (3×n) dimensional jacobian matrices of rotary speed; I_{c1}, I_{cgs} – (3×3) dimensional mass moment of inertia matrices of bough and branches "j" links mass centres respectively; g – subscript denotes branch sign; $\mathbf{q}_0$ – vector of generalised displacement of first joint – only one quotients q_1 is not equal zero; $\mathbf{q}_g$ – vector of generalised displacement of all branches joints (in this vector q_1 also is present); n – sum of number of degrees of freedom of bough and single branch respectively.
Now the expressions in curly bracket in equation (8) allow us to write the dynamic matrices in form:

$$\mathbf{D} = \left[\begin{array}{c:c:c:c} \mathbf{k} & \mathbf{a}_k & \mathbf{b}_k & \cdots \\ \hdashline \mathbf{a}_k^T & \mathbf{a} & \mathbf{0} & \cdots \\ \hdashline \mathbf{b}_k^T & \mathbf{0} & \mathbf{b} & \ddots \\ \hdashline \vdots & \vdots & \ddots & \ddots \end{array}\right] \tag{9}$$

Above presented matrix is a block – symmetric matrix, which consist of sub – matrices **k**, **a**, **b**, … and $\mathbf{a}_k$, $\mathbf{b}_k$, …. The physical interpretation of this sub – matrices is as follows:

- **k** – self inertial components of bough, it is (1×1) dimensional matrix, which k_{11} elements is expressed in form:

$$k_{(11)} = m_{c1}\sum_{i=1}^{3} J_{vc1\_i1}^2 + I_{zc1}(\sum_{i=1}^{3} J_{\omega c1\_i1} r_{c1\_i3})^2 + \sum_g \sum_{s=2}^{n} m_{cgs}\sum_{i=1}^{3} J_{vcgs\_i1}^2 + \sum_g \sum_{s=2}^{n} I_{zgs}(\sum_{i=1}^{3} J_{\omega cgs\_i1} r_{cgs\_i3})^2 \tag{10}$$

  where: J_{vc1_i1}, J_{wc1_i1}, J_{vcgs_i1}, J_{wgs_i1} – elements of jacobian matrices: linear and rotating speed of bough, linear and rotating speeds of branches respectively; $r_{c1\_i\,3}$, $r_{cgs\_i\,3}$ – $(i,3)$ elements of rotation matrix of homogenous transformation related to appropriate mass centre.
- **a**, **b**, … – square matrices in which internal diagonal quotients representing the self inertial components of branches. The quotients which lie above diagonal represent mutual inertial couplings between joints of chosen branch. This matrix components are given by:
  - diagonal components for c ≥ 2 (c – denotes columns of block matrix (9)):

$$g_{(c-1,c-1)} = \sum_{s=2}^{n}\left(m_{cgs}\sum_{i=1}^{3} J_{vcgs\_ic}^2 + I_{zgs}(\sum_{i=1}^{3} J_{\omega cgs\_ic} r_{cgs\_i3})^2\right) \tag{11}$$

- above diagonal components for r ≠ c and r ≥ 2 and c > 2 (r – denotes rows of block matrix (9)):

$$g_{(r,c)} = \sum_{s=2}^{n}\left(m_{cgs}\sum_{i=1}^{3}\prod_{j\in\{r,c\}} J_{vcgs\_ij} + I_{zgs}\prod_{j\in\{r,c\}}\sum_{i=1}^{3} J_{\omega cgs\_ij} r_{cgs\_i3}\right) \tag{12}$$

- $\mathbf{a}_k$, $\mathbf{b}_k$, … – row ((1×(n-1)) dimensional) matrices representing inertial mutual couplings between joints of branch and bough (the branch-bough inertial couplings). The components of this matrices are, for r = 1 and c ≥ 2, as follows:

$$g_{k(r,c-1)} = \sum_{s=2}^{n}\left(m_{cgs}\sum_{i=1}^{3}\prod_{j\in\{r,c\}} J_{vcgs\_ij} + I_{zgs}\prod_{j\in\{r,c\}}\sum_{i=1}^{3} J_{\omega cgs\_ij} r_{cgs\_i3}\right) \tag{13}$$

In the case of multilayer head positioning system, presented in Fig.9 (where it was assumed that it cooperates with set of two data disk), the dynamic block matrix is expressed by:

$$\mathbf{D} = \left[\begin{array}{c:cc:cc:cc:cc:c}
k_{11} & a_{k11} & a_{k12} & b_{k11} & b_{k12} & c_{k11} & c_{k12} & d_{k11} & d_{k11} & \cdots \\ \hdashline
 & a_{11} & 0 & 0 & 0 & 0 & 0 & 0 & 0 & \cdots \\
 & & a_{22} & 0 & 0 & 0 & 0 & 0 & 0 & \cdots \\ \hdashline
 & & & b_{11} & 0 & 0 & 0 & 0 & 0 & \cdots \\
 & & & & b_{22} & 0 & 0 & 0 & 0 & \cdots \\ \hdashline
 & & & & & c_{11} & 0 & 0 & 0 & \cdots \\
 & & & & & & c_{22} & 0 & 0 & \cdots \\ \hdashline
 & & & & & & & d_{11} & 0 & \\
 & sym. & & & & & & & d_{22} & \ddots \\ \hdashline
 & & & & & & & & & \ddots
\end{array}\right] \tag{14}$$

What is worth to underlining, there exists mutual inertial couplings between each joint of branches and bough – because the elements of row matrices are different from zero. However there is not inertial coupling between branches joints – this is a consequence that rotating axis of second joints (of every branch) is parallel to translation axes of third joints (of every branch). The self inertial components of bough, for multilayer kinematics chain at the point, is given by:

$$\begin{aligned} k_{11} = {} & m_{c1}a_{c1}^2 + I_{zc1} + \sum_{g\in\{a,b,c,d\}} m_{cg2}(a_1 + a_{cg2}\,c_{g2})^2 + \sum_{g\in\{a,c\}} m_{cg3}((a_1 + a_{g2}c_{g2} - a_{cg3}s_{g2})^2 + d_{g3}^2) + \\ & + \sum_{g\in\{b,d\}} m_{cg3}((a_1 + a_{g2}c_{g2} + a_{cg3}s_{g2})^2 + d_{g3}^2) \end{aligned} \tag{15}$$

where a_1, a_{c1}, a_{g2}, a_{cg2}, d_{g3} – denotes adequately: length of bough link, position of mass centre of bough, length of seconds and position of mass centre of thirds links and elongation of prismatic joints of adequate "g" branches; m_{cg2}, m_{cg3} – denotes masses of adequate branches links; s_{g2}, c_{g2} - denotes the abbreviated notation of cosine and sine functions of second joints angles of appropriate branches. The self inertial components of g matrices (for "a", "b", "c" and "d" branches) is expressed by:

$$\begin{cases} g_{11} = m_{cg2}a_{cg2}^2 + I_{zg2} + m_{cg3}(a_{g2}^2 + a_{cg3}^2) + I_{zg3} \\ g_{22} = m_{cg3} \end{cases} \tag{16}$$

where I_{zg2}, I_{zg3} – denotes adequately mass moment of inertia of appropriate branches links.
The branch-bough inertial couplings matrices components are as follows:

- for "a" and "c" branches:

$$\begin{cases} g_{k11} = -d_{g3}m_{cg3}(a_{cg3}c_{g2} + a_{g2}s_{g2}) \\ g_{k12} = -m_{cg3}(a_1 + a_{g2}c_{g2} - a_{cg3}s_{g2}) \end{cases} \tag{17}$$

- for "b" and "d" branches:

$$\begin{cases} g_{k11} = -m_{cg3}d_{g3}(-a_{cg3}c_{g2} + a_{g2}s_{g2}) \\ g_{k12} = -m_{cg3}(a_1 + a_{g2}c_{g2} + a_{cg3}s_{g2}) \end{cases} \tag{18}$$

Components of matrices for "a", "c" and "b", "d" branches differs, because the first two cooperate with top part of data disk, but the other two with bottom part of data disk.

3.2 Dynamics matrix inversion using block matrices

For dynamics block matrix inversion, one advantages may be taken of hers block structure which allows for her inversion with the help of block matrices. According to the definition of inverse matrix, we have:

$$\mathbf{D}^{-1}\mathbf{D} = \mathbf{1} \tag{19}$$

where $\mathbf{1}$ – denotes unity matrix, or:

$$\frac{adj\mathbf{D}_r}{\det \mathbf{D}_r}\mathbf{D}_r = \mathbf{1} \tag{20}$$

Multiplying then both sides of equation (20) by determinant of dynamic matrix we get following matrix equation expressed in terms of elementary sub-matrices (corresponding with bough and branches):

$$\begin{bmatrix} \mathbf{A}_{11} & \mathbf{A}_{12} & \mathbf{A}_{13} & \mathbf{A}_{14} & \mathbf{A}_{15} \\ \mathbf{A}_{21} & \mathbf{A}_{22} & \mathbf{A}_{23} & \mathbf{A}_{24} & \mathbf{A}_{25} \\ \mathbf{A}_{31} & \mathbf{A}_{32} & \mathbf{A}_{33} & \mathbf{A}_{34} & \mathbf{A}_{35} \\ \mathbf{A}_{41} & \mathbf{A}_{42} & \mathbf{A}_{43} & \mathbf{A}_{44} & \mathbf{A}_{45} \\ \mathbf{A}_{51} & \mathbf{A}_{52} & \mathbf{A}_{53} & \mathbf{A}_{54} & \mathbf{A}_{55} \end{bmatrix} \begin{bmatrix} \mathbf{k} & \mathbf{a}_k & \mathbf{b}_k & \mathbf{c}_k & \mathbf{d}_k \\ \mathbf{a}_k^T & \mathbf{a} & \mathbf{0} & \mathbf{0} & \mathbf{0} \\ \mathbf{b}_k^T & \mathbf{0} & \mathbf{b} & \mathbf{0} & \mathbf{0} \\ \mathbf{c}_k^T & \mathbf{0} & \mathbf{0} & \mathbf{c} & \mathbf{0} \\ \mathbf{d}_k^T & \mathbf{0} & \mathbf{0} & \mathbf{0} & \mathbf{d} \end{bmatrix} = \mathbf{1}\det \mathbf{D} \tag{21}$$

This equation, after multiplication give us a five sets of five matrix equations, with unknown sub-matrices $\mathbf{A}_{ij}$ of adjunction matrix. This sets of equation should be solved according to unknown $\mathbf{A}_{ij}$ sub-matrices. The exemplary set of five matrix equation – related with the first row of adjunction matrix and first column of dynamics matrix is presented below:

$$\begin{cases} \mathbf{A}_{11}\mathbf{k} + \mathbf{A}_{12}\mathbf{a}_k^T + \mathbf{A}_{13}\mathbf{b}_k^T + \mathbf{A}_{14}\mathbf{c}_k^T + \mathbf{A}_{15}\mathbf{d}_k^T = \mathbf{1}\det\mathbf{D} \\ \mathbf{A}_{11}\mathbf{a}_k + \mathbf{A}_{12}\mathbf{a} = \mathbf{0} \\ \mathbf{A}_{11}\mathbf{b}_k + \mathbf{A}_{13}\mathbf{b} = \mathbf{0} \\ \mathbf{A}_{11}\mathbf{c}_k + \mathbf{A}_{14}\mathbf{c} = \mathbf{0} \\ \mathbf{A}_{11}\mathbf{d}_k + \mathbf{A}_{15}\mathbf{d} = \mathbf{0} \end{cases} \tag{22}$$

After solving of this matrix equation (22) and the rest similar, we get (here is only the one of five sets of solution presented):

$$\begin{cases} \mathbf{A}_{11} = \det\mathbf{D}\ (\mathbf{k} - \mathbf{a}_k\mathbf{a}^{-1}\mathbf{a}_k^T - \mathbf{b}_k\mathbf{b}^{-1}\mathbf{b}_k^T - \mathbf{c}_k\mathbf{c}^{-1}\mathbf{c}_k^T - \mathbf{d}_k\mathbf{d}^{-1}\mathbf{d}_k^T)^{-1} \\ \mathbf{A}_{12} = -\det\mathbf{D}\ (\mathbf{k} - \mathbf{a}_k\mathbf{a}^{-1}\mathbf{a}_k^T - \mathbf{b}_k\mathbf{b}^{-1}\mathbf{b}_k^T - \mathbf{c}_k\mathbf{c}^{-1}\mathbf{c}_k^T - \mathbf{d}_k\mathbf{d}^{-1}\mathbf{d}_k^T)^{-1}\mathbf{a}_k\mathbf{a}^{-1} \\ \mathbf{A}_{13} = -\det\mathbf{D}\ (\mathbf{k} - \mathbf{a}_k\mathbf{a}^{-1}\mathbf{a}_k^T - \mathbf{b}_k\mathbf{b}^{-1}\mathbf{b}_k^T - \mathbf{c}_k\mathbf{c}^{-1}\mathbf{c}_k^T - \mathbf{d}_k\mathbf{d}^{-1}\mathbf{d}_k^T)^{-1}\mathbf{b}_k\mathbf{b}^{-1} \\ \mathbf{A}_{14} = -\det\mathbf{D}\ (\mathbf{k} - \mathbf{a}_k\mathbf{a}^{-1}\mathbf{a}_k^T - \mathbf{b}_k\mathbf{b}^{-1}\mathbf{b}_k^T - \mathbf{c}_k\mathbf{c}^{-1}\mathbf{c}_k^T - \mathbf{d}_k\mathbf{d}^{-1}\mathbf{d}_k^T)^{-1}\mathbf{c}_k\mathbf{c}^{-1} \\ \mathbf{A}_{15} = -\det\mathbf{D}\ (\mathbf{k} - \mathbf{a}_k\mathbf{a}^{-1}\mathbf{a}_k^T - \mathbf{b}_k\mathbf{b}^{-1}\mathbf{b}_k^T - \mathbf{c}_k\mathbf{c}^{-1}\mathbf{c}_k^T - \mathbf{d}_k\mathbf{d}^{-1}\mathbf{d}_k^T)^{-1}\mathbf{d}_k\mathbf{d}^{-1} \end{cases} \tag{23}$$

The obtained results should be divided by determinant of dynamic matrix. It is easy to spot that in the set of solutions appears common quotients, which since then will be called as heading matrix (element) $\mathbf{k}_1$:

$$\mathbf{k}_1 = (\mathbf{k} - \mathbf{a}_k\mathbf{a}^{-1}\mathbf{a}_k^T - \mathbf{b}_k\mathbf{b}^{-1}\mathbf{b}_k^T - \mathbf{c}_k\mathbf{c}^{-1}\mathbf{c}_k^T - \mathbf{d}_k\mathbf{d}^{-1}\mathbf{d}_k^T)^{-1} \tag{24}$$

The heading matrix is present also in diagonal elements of calculated adjunction matrix:

$$\begin{cases} \mathbf{A}_{22} = \det\mathbf{D}\ (\mathbf{a} - \mathbf{a}_k^T(\mathbf{k}_1^{-1} + \mathbf{a}_k\mathbf{a}^{-1}\mathbf{a}_k^T)^{-1}\mathbf{a}_k)^{-1} \\ \mathbf{A}_{33} = \det\mathbf{D}\ (\mathbf{b} - \mathbf{b}_k^T(\mathbf{k}_1^{-1} + \mathbf{b}_k\mathbf{b}^{-1}\mathbf{b}_k^T)^{-1}\mathbf{b}_k)^{-1} \\ \mathbf{A}_{44} = \det\mathbf{D}\ (\mathbf{c} - \mathbf{c}_k^T(\mathbf{k}_1^{-1} + \mathbf{c}_k\mathbf{c}^{-1}\mathbf{c}_k^T)^{-1}\mathbf{c}_k)^{-1} \\ \mathbf{A}_{55} = \det\mathbf{D}\ (\mathbf{d} - \mathbf{d}_k^T(\mathbf{k}_1^{-1} + \mathbf{d}_k\mathbf{d}^{-1}\mathbf{d}_k^T)^{-1}\mathbf{d}_k)^{-1} \end{cases} \tag{25}$$

After division the equation (25) by determinant of dynamic matrix, the diagonal elements of inverted block matrix are as follows:

$$\begin{cases} \mathbf{a}_1 = (\mathbf{a} - \mathbf{a}_k^T(\mathbf{k}_1^{-1} + \mathbf{a}_k\mathbf{a}^{-1}\mathbf{a}_k^T)^{-1}\mathbf{a}_k)^{-1} \\ \mathbf{b}_1 = (\mathbf{b} - \mathbf{b}_k^T(\mathbf{k}_1^{-1} + \mathbf{b}_k\mathbf{b}^{-1}\mathbf{b}_k^T)^{-1}\mathbf{b}_k)^{-1} \\ \mathbf{c}_1 = (\mathbf{c} - \mathbf{c}_k^T(\mathbf{k}_1^{-1} + \mathbf{c}_k\mathbf{c}^{-1}\mathbf{c}_k^T)^{-1}\mathbf{c}_k)^{-1} \\ \mathbf{d}_1 = (\mathbf{d} - \mathbf{d}_k^T(\mathbf{k}_1^{-1} + \mathbf{d}_k\mathbf{d}^{-1}\mathbf{d}_k^T)^{-1}\mathbf{d}_k)^{-1} \end{cases} \tag{26}$$

When all results will be collected together and written in matrix form, it forms the inverted block matrix of multilayer head positioning system consisted of four branches (which is presented in Fig. 9):

$$\mathbf{D}^{-1} = \left[\begin{array}{c:c:c:c:c} \mathbf{k}_1 & -\mathbf{k}_1\mathbf{a}_k\mathbf{a}^{-1} & -\mathbf{k}_1\mathbf{b}_k\mathbf{b}^{-1} & -\mathbf{k}_1\mathbf{c}_k\mathbf{c}^{-1} & -\mathbf{k}_1\mathbf{d}_k\mathbf{d}^{-1} \\ \hdashline & \mathbf{a}_1 & \mathbf{a}^{-1}\mathbf{a}_k^T\mathbf{k}_1\mathbf{b}_k\mathbf{b}^{-1} & \mathbf{a}^{-1}\mathbf{a}_k^T\mathbf{k}_1\mathbf{c}_k\mathbf{c}^{-1} & \mathbf{a}^{-1}\mathbf{a}_k^T\mathbf{k}_1\mathbf{d}_k\mathbf{d}^{-1} \\ \hdashline & & \mathbf{b}_1 & \mathbf{b}^{-1}\mathbf{b}_k^T\mathbf{k}_1\mathbf{c}_k\mathbf{c}^{-1} & \mathbf{b}^{-1}\mathbf{b}_k^T\mathbf{k}_1\mathbf{d}_k\mathbf{d}^{-1} \\ \hdashline & & & \mathbf{c}_1 & \mathbf{c}^{-1}\mathbf{c}_k^T\mathbf{k}_1\mathbf{d}_k\mathbf{d}^{-1} \\ \hdashline sym. & & & & \mathbf{d}_1 \end{array}\right] \tag{27}$$

If head positioning system, in point, will be equipped with three branches the block matrix presented by equation (27) shrinks to the first four block rows and block columns. Similarly when head positioning system will consist only with two branches, then inverted block matrix will decreased to three block rows and block columns. The relation between numbers of branches of multilayer head positioning system and construction of inversed dynamic block matrix in illustrative way is presented in Fig. 10.

four branches

three branches

two branches

one branch

$$\mathbf{D}^{-1} = \left[\begin{array}{c:c:c:c:c} \boxed{\mathbf{k}_1} & -\mathbf{k}_1\mathbf{a}_k\mathbf{a}^{-1} & -\mathbf{k}_1\mathbf{b}_k\mathbf{b}^{-1} & -\mathbf{k}_1\mathbf{c}_k\mathbf{c}^{-1} & -\mathbf{k}_1\mathbf{d}_k\mathbf{d}^{-1} \\ \hdashline & \mathbf{a}_1 & \mathbf{a}^{-1}\mathbf{a}_k^T\mathbf{k}_1\mathbf{b}_k\mathbf{b}^{-1} & \mathbf{a}^{-1}\mathbf{a}_k^T\mathbf{k}_1\mathbf{c}_k\mathbf{c}^{-1} & \mathbf{a}^{-1}\mathbf{a}_k^T\mathbf{k}_1\mathbf{d}_k\mathbf{d}^{-1} \\ \hdashline & & \mathbf{b}_1 & \mathbf{b}^{-1}\mathbf{b}_k^T\mathbf{k}_1\mathbf{c}_k\mathbf{c}^{-1} & \mathbf{b}^{-1}\mathbf{b}_k^T\mathbf{k}_1\mathbf{d}_k\mathbf{d}^{-1} \\ \hdashline & & & \mathbf{c}_1 & \mathbf{c}^{-1}\mathbf{c}_k^T\mathbf{k}_1\mathbf{d}_k\mathbf{d}^{-1} \\ \hdashline sym. & & & & \mathbf{d}_1 \end{array}\right]$$

Fig. 10. Increase of inversed dynamic block matrix dimension v. branch number increase

And also the heading matrix change when number of branches will change. When multilayer head positioning system is equipped with three branches from equation (24) disappears the last term, but when he is equipped with two branches - disappears two last terms, etc. The relation between numbers of branches of multilayer head positioning system and construction of heading matrix (elements) is presented in Fig.11.

$$\mathbf{k}_1 = (\overbrace{\overbrace{\overbrace{\overbrace{\boxed{\mathbf{k}} - \boxed{\mathbf{a}_k\mathbf{a}^{-1}\mathbf{a}_k^T}}^{\text{one branch}} - \boxed{\mathbf{b}_k\mathbf{b}^{-1}\mathbf{b}_k^T}}^{\text{two branches}} - \boxed{\mathbf{c}_k\mathbf{c}^{-1}\mathbf{c}_k^T}}^{\text{three branches}} - \boxed{\mathbf{d}_k\mathbf{d}^{-1}\mathbf{d}_k^T}}^{\text{four branches}})^{-1}$$

Fig. 11. Increase of heading matrix components v. branch number increase

The dimension of heading matrix not changing versus increase of number of branches, her size is defined when dynamics block matrix is formulated and always is (1×1). Only numbers of components in equation (24) changes upon branch numbers change.
As my be observed in equation (27) and Fig.10 the rest elements of inversed dynamic matrix my by easily derived. The heading matrix in every block columns (except the first one) of inversed dynamic block matrix is right hand multiplied by product of two matrices - inversed self inertial components matrix of the branch (given by general equation (11) and (12)) and transposed branch-bough inertial couplings matrix (given by general equation (13)), which actually lie in desired column before dynamics matrix inversion.
Every block rows (except the first one) of inverted dynamic block matrix should be left hand multiplied by product of two matrices - inversed self inertial matrix of branch and transposed branch-bough inertial couplings matrix, which actually lie in desired column before dynamics matrix inversion. In illustrative way the deriving the rest components of inversed dynamics block matrix of multilayer head positioning system is presented in Fig.12.

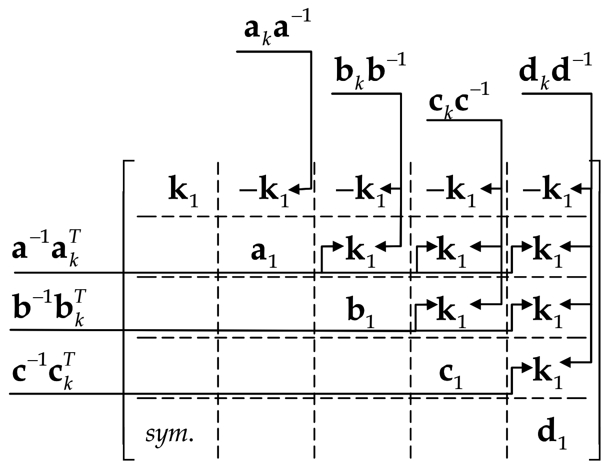

Fig. 12. Graphical method for deriving the components of inversed dynamics block matrix

4. Conclusion

The formulated dynamics block matrix of multilayer head positioning system consist of sub-matrixes which are related directly with structure of his kinematic chain. The dynamic block matrix consists of: bough self inertial matrix, self inertial matrix of branches, branch-bough inertial coupling matrix. The bough self inertial matrix is always one by one dimensional. But this matrix is very sensitive for increase of numbers of branches, adding one new branch into kinematic chains it result in two new components in equation (10). The self inertial matrices of branches are square, symmetrical matrices which may be very often diagonal matrices (Trawiński, 2007), (Trawiński, 2008). The dimension of these matrices always equals the branches number degrees of freedom. The branch-bough inertial couplings matrices are row matrices with numbers of elements equalling the numbers of degrees of freedom of chosen branches. The presented block matrices of multilayer head positioning system may be easily inverted by methods presented in chapter 3.2. In inverted form of dynamic block matrix the common heading matrix is present and the rest of inverted matrix element may be expressed in terms of them. Assumed and presented division of dynamics matrix into block matrix is natural and strictly related with structure of kinematic chain. In some special cases of multilayer head positioning system it is possible to divide dynamics matrix into very small block matrices – one by one dimensional. It usually happens when the number of degrees of freedom equals two. For highest numbers of branch degrees of freedom the division of dynamics matrix, which assure smallest possible dimensions of sub-matrices, is that presented in this chapter. One should be stressed that sizes of sub-matrices of dynamics block matrices influence on numbers of algebraic operations which have to be made during inversion process. This problem is discussed in (Trawiński, 2009).

5. References

Chen, T.-L. & Horowitz, R. (2001). Design, fabrication and dynamic analysis of a PZT-actuated silicon suspension, *Proceedings of American Control Conference*, pp. 1235 - 1240, Arlington, June 2001,

Hong, E.-J.; Kim, W.-S. & Lee, H. S. (2006). Design modification of micro-actuator to improve shock resistance of HDD, *Proceedings of Asia-Pacific Magnetic Recording Conference*, p.1-2, ISBN 1-4244-0863-6, Singapore, December 2006,

Huang, X.; Horowitz, R. & Li, Y. (2005). Design and analysis of robust track-following controllers for dual-stage servo system with an instrumented suspension, *Proceedings of American Control Conference*, pp.1126-1131, June 2005, Portland, USA,

Huang, X. & Horowitz, R. (2005). Robust controller design of a dual-stage disk drive servo system with an instrumented suspension, *IEEE Transacions on Magnetics*, Vol.41, No. 8, August 2005, pp. 2406-2413,

Jiang, M.; Bordson, T.; Gunderson, N. & Lawrence, B. (2007). HDD micro-actuator reliability study, *Proceedings of Reliability and Maintainability Symposium RAMS '07*, ISBN 0-7803-9766-5, pp. 254-258, January 2007, Orlando, FL,

Koganezawa, S. & Hara, T. (2001). Development of shear-mode piezoelectric microactuator for precise head positioning, *Fujitsu Scientific & Technical Journal*, Vol. 37, No.2, December 2001, pp. 212-219,

Ohno, K. & Horowitz, R. (2005). A pivot nonlinearity compensation by use of variable structure estimator for hard disk drives, *Microsystem Technologies*, Vol. 11, No. 8, August 2005, pp. 702–710, ISSN 0946-7076

Rotunno, M.; Oboe, R. & de Callafon, R. A. (2006). Modeling product variations in hard disk drive micro-actuator suspensions, *Microsystem Technologies*, Vol.12, No. 9, August 2006, pp.803-813, ISSN: 0946-7076,

Sarajlic, E.; Yamahata, C.; Cordero, M. & Fujita, H. (2009). Electrostatic rotary stepper micromotor for skew angle compensation in hard disk drive, *IEEE 22nd International Conference on Micro Electro Mechanical Systems*, pp.1079 – 1082, January 2009,

Sugaya, S. (2006). Trends in Enterprise hard disk drives, *Fujitsu Scientific & Technical Journal*, Vol. 42, No.1, January 2006, pp. 61-71,

Suh, S.-M.; Chung, C. C. & Lee, S.-H. (2001). Discrete-time LQG/LTR dual-stage controller design in magnetic disk drives, *IEEE Transactions on Magnetics,* Vol. 37, No.4, July 2001, pp.1891-1895,

Schultz, B. E. (2007). Thermal Fly-height Control (TFC) Technology in Hitachi Hard Disk Drives, White Paper, Hitachi Global Storage Technologies 2007, Trawiński, T. (2007). Mathematical model of head actuator of hard-disk drive with passive joint, *Electromotion*, Vol.14, No.1, January-March 2007, p.32-37, ISSN 1223-057X,

Trawiński, T. & Kluszczyński, K. (2008). Mathematical modelling of double-shell hard disk drive positioning system regarded as manipulator, *Electrical Review*, Vol.84, No. 6, June 2008, pp.153-156, ISSN 0033-2097, (in polish),

Trawiński, T. (2008). Double layer head positioning system with five degrees of freedom, *XVIII Symposium PTZE*, pp.101-102, ISBN 978-83-7373-038-0, Zamość, Poland, Jun 2008, Polish Society of Applied Electromagnetism, Warszawa,

Trawiński, T. (2009). Inversion method of matrices with chosen structure with help of block matrices, *Electrical Review*, Vol. 85, No. 6, June 2009, pp. 98-101, ISSN 0033-2097, (in polish),

Wang, Z. & Krishnamurthy, P. (2006). A novel recursive filtering approach to estimate repeatable run-out (RRO) disturbance in HDD, *Proceedings of the 2006 American Control Conference*, pp. 2011-2015, ISBN 1-4244-0209-3, Minneapolis, Minnesota, USA, June 2006,

Robot Manipulators New Achievements

Edited by Aleksandar Lazinica and Hiroyuki Kawai

ISBN 978-953-307-090-2
Hard cover, 718 pages
Publisher InTech
Published online 01, April, 2010
Published in print edition April, 2010

Robot manipulators are developing more in the direction of industrial robots than of human workers. Recently, the applications of robot manipulators are spreading their focus, for example Da Vinci as a medical robot, ASIMO as a humanoid robot and so on. There are many research topics within the field of robot manipulators, e.g. motion planning, cooperation with a human, and fusion with external sensors like vision, haptic and force, etc. Moreover, these include both technical problems in the industry and theoretical problems in the academic fields. This book is a collection of papers presenting the latest research issues from around the world.